Mechatronics 24 (2014) 1059–1070

Contents lists available at ScienceDirect

Mechatronics

journal homepage: www.elsevier.com/locate/mechatronics

Development of a totally active magnetically suspended gyro

Tomohiro Akiyama, Takeshi Mizuno *, Masaya Takasaki, Yuji Ishino, Kyosuke Obara

Department of Mechanical Engineering, Saitama University, Shimo-okubo 255, Sakura-ku, Saitama 338-8570, Japan

ARTICLE INFO

Article history:
Received 8 October 2013
Accepted 24 June 2014
Available online 26 July 2014

Keywords:
Gyroscopic sensor
Angular velocity measurement
Magnetic levitation
Six-degrees-of-freedom control
Unbalance compensation

ABSTRACT

A magnetically suspended gyro (MSG) is developed and its performances is estimated. In the MSG, a disk-type rotor is connected to a synchronous motor through a fluid bearing and the motor is fixed to the frame of the floator. The floator is suspended by magnetic force without any mechanical contact so that highly accurate measurement is possible. In accordance with this concept, a three-degrees-of-freedom (DOF) active MSG was developed. However, because of poor damping in the passive suspension and the low resolution of the displacement sensors, the measurement accuracy was relatively low. To solve these problems, a six-DOF (totally) active MSG is designed and fabricated. The frame of this gyro is an octagonal. The motion of the frame is controlled by eight electromagnets. The performance of the gyro is evaluated through measurement of the double-axis angular velocity. The advantages of totally active suspension are investigated. Sufficient damping rapidly reduces the influence of disturbances. Then, the influence of sensor noise is examined. The results of this examination show that the accuracy of the angular velocity measurement is improved by using highly sensitive displacement sensors. Next, the dynamic range is measured. This experiment shows that the MSG can provide precise angular velocity measurement in a low-frequency region.

1. Introduction

Gyroscopic sensors (gyros) measure kinematical variables of a rigid body based on inertial effects caused by rotational motion. Rate gyros measure angular velocity. They are used in various fields, such as inertial navigation, homing, and attitude control. Highly accurate, compact, and low-cost gyros are required to achieve sophisticated motion control of robots and unmanned airplanes.

According to the detection principle, rate gyros are classified into three main categories: optical, vibrating, and rotating gyros. Optical gyros utilize the Sagnac effect [1]. They are generally used for applications that require high accuracy, such as inertial navigation systems for airplanes. However, they are rather expensive. Vibrating gyros utilize the Coriolis force acting on vibrating proof mass. Most micro electro mechanical systems (MEMS) gyros are based on this principle. They are mostly used for compact and low-cost applications such as video cameras, controllers, and smartphones. Although most-advanced ones are applicable even in aircraft navigation system and satellites [2], most of them have not been used in high-performance applications. Rotating gyros utilize angular momentum of a spinning rotor. Although the rotor mass is small, the detection sensitivity increases with spinning rate. Therefore, they have the potential to achieve high accuracy. However, they are prone to measurement error caused by friction in the gimbal mechanism that guides the rotations of the rotor about the axes that are orthogonal to the spinning axis.

Magnetic suspension technology can essentially eliminate mechanical friction [3]. One promising application of this technology is to suspend a rotating body (rotor) directly, which is referred to as magnetic bearing [4]. A rotating gyro using an active magnetic bearing (AMB), called AMB-based gyro, was proposed and fabricated previously [5]. In this gyro, the rotor was directly suspended by electromagnets (EMs). The AMB-based gyro provided good performance. However, the design of the rotor was limited by the necessity of lamination in the rotor.

To overcome this problem, a magnetically suspended gyro (MSG) has been proposed [6]. In this gyro, a floator, including a motor-driven rotor, is suspended magnetically instead of the rotor. Because the floator does not spin at high speed, no lamination of the EM targets is required to reduce eddy-current loss. In addition, it has the potential to use any rotating machine as a gyro. Therefore, the MSG is more suitable for miniaturization and low-cost application than the AMB-based gyro. A proto-type MSG was fabricated in which only three degrees of freedom (DOF) of the floator were actively controlled by EM. However, the three-DOF active MSG had several problems. First, the floator's other DOF

* Corresponding author. Tel.: +81 48 858 3455; fax: +81 48 858 3712.
E-mail address: mizar@mech.saitama-u.ac.jp (T. Mizuno).

http://dx.doi.org/10.1016/j.mechatronics.2014.06.004
0957-4158/

Nomenclature

x, y, z	relative displacements of the floator to the stator along the x-, y-and z-axes (m)
$\theta_x, \theta_y, \theta_z$	relative angular displacements of the floator to the stator along the x-, y-and z-axes (rad)
x_f, y_f, z_f	absolute displacements of the floator along the x-, y- and z-axes (m)
ψ_x, ψ_y, ψ_z	absolute angular displacements of the floator about the x-, y-and z-axes (rad)
x_s, y_s, z_s	absolute displacements of the stator along the x-, y-and z-axes (m)
$\varphi_x, \varphi_y, \varphi_z$	absolute angular displacements of the stator about the x-, y-and z-axes (rad)
F_j	force of the jth electromagnet (N)
F_s	steady force of electromagnets 1–4 (N)
K_i	coefficient of electromagnets 1–4 (N/A)
K_d	coefficient of electromagnets 1–4 (N/m)
F_{sa}	steady force of electromagnets 5 and 8 (N)
K_{ia}	coefficient of electromagnets 5 and 8 (N/A]
K_{da}	coefficient of electromagnets 5 and 8 (N/m)
F_{sb}	steady force of electromagnets 6 and 7 (N)
K_{ib}	coefficient of electromagnets 6 and 7 (N/A)
K_{db}	coefficient of electromagnets 6 and 7 (N/m)
u_j	control input (A)
d_j	gap between the jth electromagnet and the floator (m)
l	distance of electromagnets from the x-axis (m)
l_z	deflected displacement of EMs 5–8 from the symmetrical axis (m)
u_x, u_y, u_z	control inputs along the x-, y-and z-axes (A)
$u_{\theta x}, u_{\theta y}, u_{\theta z}$	control inputs about the x-, y-and z-axes (A)
F_x, F_y, F_z	control forces along the x-, y-and z-axes (N)
T_x, T_y, T_z	control torques about the x-, y-and z-axes (Nm)
m	mass of the floator (kg)
I_r	transverse moment of inertia of the floator (kgm^2)
I_{rz}	polar moment of inertia of the floator (kgm^2)
I_a	principal axis of inertia moment of the floator (kgm^2)
ω	angular velocity of the rotor about principal axis (rad/s)
I_p	polar moment of inertia of the floator (kgm^2)
ε, α	amounts of rotation of static unbalance (–)
τ, β	amounts of rotation of dynamic unbalance (–)
w_x, w_y	unbalance forces (m/s^2)
$w_{\theta x}, w_{\theta y}$	unbalance forces (rad/s^2)
a_x, a_y, a_z	coefficients related to negative stiffness (1/s^2)
$a_\theta, a_{\theta z}$	coefficients related to negative stiffness (1/s^2)
a_1, a_2	coefficients related to negative stiffness (1/s^2)
b_x, b_y, b_z	acceleration coefficient (m/As^2)
$b_\theta, b_{\theta z}$	angular acceleration coefficient (rad/As^2)
a_k	value describing effect of gyroscopic action to rotor (rad/s)
Ψ_x, Ψ_y	the Laplace transformed $\dot{\varphi}_x$ (rad/s)
$U_{\theta x}, U_{\theta y}$	the Laplace transformed $u_{\theta x}$ (A)
$\hat{\dot{\varphi}}_x, \hat{\dot{\varphi}}_y$	estimated angular velocities (rad/s)
$\hat{\Psi}_x, \hat{\Psi}_y$	the Laplace transformed $\hat{\dot{\varphi}}_x$ (rad/s)
k_{px}, k_{py}, k_{pz}	proportional gains (A/m)
$k_{p\theta}, k_{p\theta z}$	proportional gains (A/rad)
k_{dx}, k_{dy}, k_{dz}	differential gains (As/m)
$k_{d\theta}, k_{d\theta z}$	differential gains (As/rad)
k_{ix}, k_{iy}, k_{iz}	integral gains (A/ms)
$k_{i\theta}, k_{i\theta z}$	integral gains (A/rads)
k_c	cross feedback gain (As/rad)
k_{cx}	cross feedback gain (m/rad)
$k_{c\theta z}$	cross feedback gain (rad/m)

were passively supported by the repulsive force between permanent magnets with same polarity. Poor damping in the passive suspension reduced the measurement accuracy. Second, because the sensors of floator displacement had low sensitivity, the estimation of angular velocity was inaccurate.

To solve these problems, a six-DOF (totally) active MSG has been developed and fabricated [7,8]. In this gyro, all the motions of the floator are actively controlled with high-sensitivity displacement sensors. These displacement sensors are the same as those used in the three-DOF active MSG, but the operating ranges are different.

In this paper, double-axis angular velocity is measured and the performance of the totally active MSG is evaluated in comparison with the three-DOF active MSG. This study demonstrates that the accuracy of angular velocity measurement is improved in the totally active MSG.

2. Magnetically suspended gyro

2.1. Three-DOF active MSG

A three-DOF active MSG (shown in Fig. 1) was developed [6]. The floator is rectangular. The translation in the z-axis direction and the rotations about the x- and y-axes of the floator to the stator are actively controlled by EMs. In contrast, the translation in the x- and y-axes and the rotation about the z-axis are passively supported by the repulsive force between permanent magnets with the same polarity.

Double-axis angular velocity was measured with this apparatus. The results demonstrated that the fabricated MSG could detect the angular velocities. However, because of poor damping in the passive suspension, measurement with the three-DOF active MSG was not very accurate.

2.2. Totally active MSG

A photo and a schematic view of the fabricated MSG are shown by Fig. 2. The apparatus is composed of a stator and a floator. The stator is installed with EMs and displacement sensors. A synchronous motor with a rotating disk rotor is fixed in the floator.

A new design of floator is shown by Fig. 3. The floator is octagonal. An octagonal shape has a lower moment of inertia than a rectangular floator, which makes gyroscopic precession more visible. The fabricated floator is shown by Fig. 4.

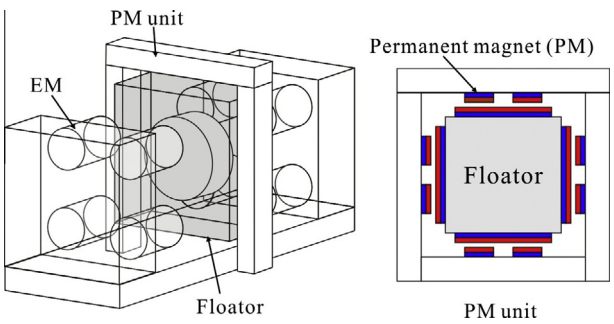

Fig. 1. Schematic view of three-DOF active MSG.